ELSEVIER

Biochimica et Biophysica Acta 1329 (1997) 124–138

BIOCHIMICA ET BIOPHYSICA ACTA
BBA

The headgroup orientation of dimyristoylphosphatidylinositol-4-phosphate in mixed lipid bilayers: a neutron diffraction study

Jeremy P. Bradshaw [a], Richard J. Bushby [b,*], Colin C.D. Giles [b], Martin R. Saunders [c], Anand Saxena [d]

[a] *Department of Preclinical Veterinary Sciences, Royal (Dick) School of Veterinary Science, University of Edinburgh, Summerhall, Edinburgh, UK*

[b] *School of Chemistry, University of Leeds, Woodhouse Lane, Leeds LS2 9JT, UK*

[c] *SmithKline Beecham Pharmaceuticals, The Frythe, Welwyn, Herts., UK*

[d] *Biology Department, Brookhaven National Laboratory, Upton, Long Island, NY, USA*

Received 21 January 1997; revised 14 April 1997; accepted 15 April 1997

Abstract

The trisodium salt of dimyristoylphosphatidylinositol-4-phosphate (DMPI-4P) has been synthesised specifically deuterated at particular sites in the headgroup. These materials have been used in neutron diffraction experiments, which successfully located the position (depth) of each of these deuterated sites to within ± 0.5 Å in a mixed model membrane (a 1:1 molar mixture of DMPI-4P with dimyristoyl-phosphatidylcholine, DMPC, in the L_α phase, hydrated to the level of 28 water molecules per lipid molecule). The diffracted intensities were measured at four different D_2O/H_2O ratios and six orders of diffraction were obtained. These data sets, in conjunction with computer modelling, have been used to determine the orientation of the inositol ring of DMPI-4P, localising each vertical H–H distance to within approximately ± 0.03 Å. The orientation of the inositol ring is found to be one in which the C5 hydroxyl is extended out into the aqueous medium. This is, therefore, the most accessible site for water-borne reagents. This may be significant for the important pathway leading from PI-4P to PI-4,5P_2. On the assumption that the P/ODAG bond is orientated parallel to the bilayer normal, these results are consistent with two possible conformations for the portion of the headgroup connecting the diacylglycerol to the inositol ring. Distinction between these two is difficult, but one may be favoured since the other involves close atom–atom contacts. © 1997 Elsevier Science B.V.

Keywords: Neutron diffraction; Dimyristoylphosphatidylinositol-4-phosphate; Biomembrane; Synthesis; Headgroup orientation

1. Introduction

The physiological roles of the phosphoinositides [1] have been well documented. They include secondary messenger roles in cellular [2] and insulin [3] signalling, and also the covalent attachment of proteins to the surface of the plasma membrane [4]. The most well-known of these processes is the involvement of phosphatidylinositol-4,5-biphosphate (PI-4,5P_2) in cellular signalling. Phosphatidylinositol (PI)

* Corresponding author. Fax: (44) (113) 233-6565.

PII S0005-2736(97)00093-X

exists in equilibrium with phosphatidylinositol-4-phosphate (PI-4P) and the 4,5-biphosphate derivative (PI-4,5P_2), courtesy of a series of selective phosphorylation and dephosphorylation enzymes. Hydrolysis of PI-4,5P_2 by a PI specific phospholipase C yields the secondary messengers inositol-1,4,5-triphosphate and diacylglycerol (DAG). In order to understand these processes, and the mechanisms of the enzymes involved, it would be of great benefit if the position and orientation of the inositol ring of the phosphoinositides in membranes could be determined.

Previous attempts to determine the orientation of the headgroup of inositol lipids by high resolution ^{1}H-NMR [5] and broad band ^{2}H-NMR [6] spectroscopy have failed to produce conclusive results. The failure of ^{2}H-NMR, a technique that has worked so well for other lipids, is a consequence of the fact that there are five parallel axial C–D bonds in the inositol ring. This degeneracy means that the ^{2}H-NMR spectra contain insufficient information to fix its orientation [6]. In this paper, we show that the problem can be solved by neutron diffraction.

Diffraction techniques have long been used to determine structural properties of molecules. Neutron diffraction has several important advantages over X-ray diffraction, the most significant of which is that neutrons are scattered differently by different isotopes of the same element. This allows neutron diffraction to be used to locate sites of isotopic labels within the structure to a high degree of accuracy. The most often used isotopic replacement method relies on hydrogen/deuterium exchange, which results in large changes in neutron scattering density with a minimal perturbation in the structure. The technique has been shown to be extremely sensitive, and has been used to study the conformational behaviour of other phospholipids [7], also to determine the nature of the interactions between phospholipids and integral membrane proteins in biomembranes [8]. We have employed neutron diffraction of specifically deuterated phosphoinositides, in conjunction with computer modelling techniques, to determine the orientational behaviour of the inositol ring of the phosphoinositides [1]. In particular, in this publication, we detail the method used and address the headgroup orientational behaviour of DMPI-4P in mixed (50:50 molar ratio) membranes with dimyristoylphosphatidylcholine (DMPC).

2. Materials

2.1. Synthesis of DMPI-4P

The phosphoinositides only comprise a small fraction of natural membranes and, due to the polyunsaturated nature of the acyl chains, these natural materials are unstable and are prone to oxidation. The deuterated analogues required for neutron diffraction experiments are not commercially available. From either standpoint, a total synthesis of the phosphoinositides was essential. Sodium DMPI-4P was synthesised essentially according to the method of Ward and Young [9,10], but with some modifications. The published procedure produced the ammonium salt of the dipalmitoyl derivative, but could easily be modified to produce the *sodium* salt of the *dimyristoyl* analogue. The final stages of the synthesis are shown in Scheme 1. Ward and Young's procedure also used *N*,*N*-diisopropyl-di-*O*-ethylphosphoramidite as the phosphitylating agent. We found that *N*,*N*-diisopropyl-di-*O*-benzylphosphoramidite was better for this purpose. This reagent was prepared by reaction of freshly prepared lithium diisopropylamide with phosphorous trichloride, followed by reaction with benzyl alcohol, using *N*,*N*-diisopropylethylamine as a base [11–13]. Coupling of *N*,*N*-diisopropyl-di-*O*-benzylphosphoramidite with (**2**) was achieved using tetrazole as a catalyst. The phosphitylated intermediate was oxidised in situ using *m*-chloroperoxybenzoic acid (*m*CPBA) to produce (**3**). Deprotection was achieved according to the method outlined by Ward and Young [10], producing the ammonium salt of the product. Unfortunately, ^{1}H-NMR (400 MHz) (overnight acquisition in CD_3OD) indicated that there was significant contamination from a closely related product. TLC of the product proved difficult, as the material associated with any free calcium and precipitated on the baseline. However, TLC analysis could be performed using the method of Gonzalez-Sastre et al. [14] (oxalate to remove all traces of calcium), and this indeed showed the product to be a mixture of two entities. Separation of the mixture could be achieved by chromatography, using a Ca^{2+}-free stationary phase, or by repeated reprecipitation of the product from a concentrated aqueous solution by the addition of methanol. In either case, the product was dried under high vacuum for 1 week. Elemental

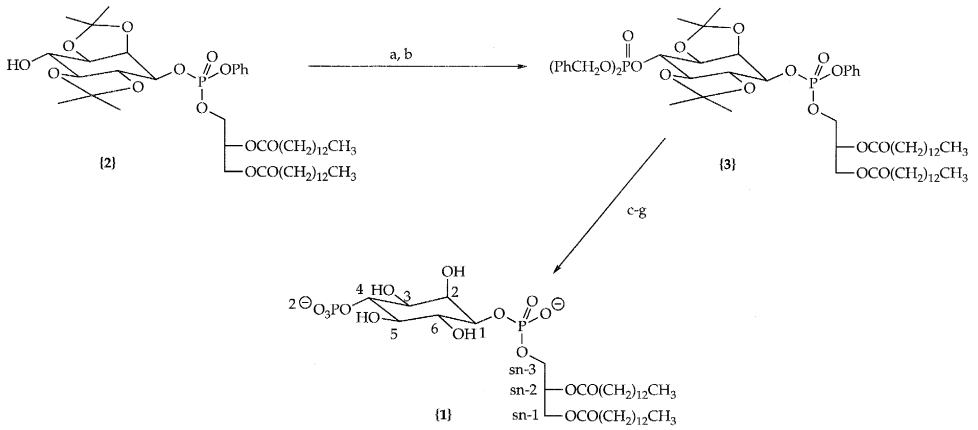

Scheme 1. Final stages in the synthesis of the sodium salt of DMPI-4P. Reagents: a, $(PhCH_2O)_2NPr^i_2$/tetrazole; b, *m*-chloroperbenzoic acid; c, $H_2/PtO_2/EtOH/EtOAc/50$ p.s.i./4 h/25°C; d, H_2O/16 h; e, NH_3/H_2O; f, chromatograph or reprecipitation; g, Na^+ ion exchange.

analysis showed the product to be a tetrahydrate: $C_{37}H_{69}Na_3O_{16}P_2 \cdot 4H_2O$. ^{1}H-NMR (400 MHz) (overnight acquisition in CD_3OD) showed a single product. The portion of the spectrum relating to the glycerol backbone and the inositol headgroup agreed with published spectra of the natural material [15].

2.2. Synthesis of deuterated analogues

To act as probes during the neutron diffraction studies, various specifically deuterated analogues of DMPI-4P were required. Myo-inositol deuterated in the 2-position (d_2), and material which had all six inositol sites deuterated (d_{1-6}) were prepared as described previously [6], and these were used as starting materials for the synthesis of DMPI-4P(d_2) and DMPI-4P(d_{1-6}) respectively. Material that was half deuterated in the 4-position and half in the 6-position was achieved according to Scheme 2. Treatment of myo-inositol with concentrated nitric acid produced 4(6)-myo-inosose in 13% yield [16]. This was reduced using 2.5% Na/Hg amalgam in D_2O [17]. This reaction produced a 60:40 mixture of myo- and epi-inositol, respectively. The pure $d_{4,6}$-myo-inositol was obtained by fractional crystallisation of a concentrated aqueous solution (3–4 parts H_2O) by addition of glacial acetic acid. The pure $d_{4,6}$-myo-inositol was

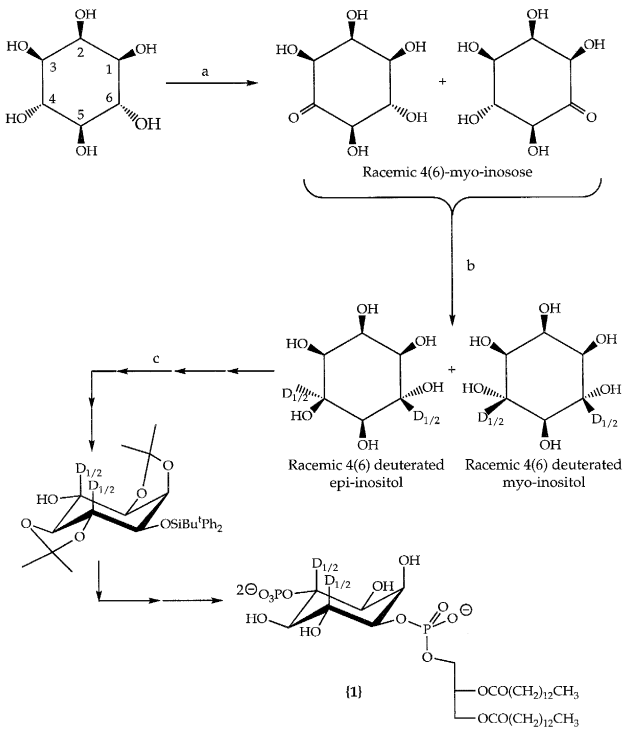

Scheme 2. Outline of the synthesis of the sodium salt of DMPI-4P partially deuterated at positions 4 and 6 of the inositol ring. Reagents: a, HNO_3; b, Na–Hg/D_2O/AcOD; c, separate protect and resolve.

obtained by filtration and then washing with ethanol. Many other methods of reductively deuterating the inosose were investigated, but none proved better than this simple route [18].

Deuteration of a reference site in the glycerol backbone was also necessary. The reference site chosen was the *sn*-3 position. Deuteration of this site was achieved by formation of the 1,2-isopropylidene-*sn*-glyceraldehyde, which was made according to the method of Jackson [19]. The glyceraldehyde was subsequently reduced using lithium aluminium deuteride in tetrahydrofuran, to produce the $d_{sn\text{-}3}$ 1,2-isopropylidene-*sn*-glycerol, which was used for the synthesis of $d_{sn\text{-}3}$ di-myristoyl diacylglycerol [9].

3. Experimental procedures

3.1. Synthesis

3.1.1. N,N-diisopropyl-di-O-benzylphosphoramidite

To a cooled (ice/water bath) solution of dry diisopropylamine (2.4 ml, 17.1 mmol) in dry diethyl ether (23.6 ml), under an atmosphere of nitrogen, a solution of *n*-butyllithium in hexanes (11 ml, 1.6 M) was added. The reaction mixture was allowed to warm to room temperature and was stirred for an additional hour. The reaction mixture was transferred via cannula into a cooled (−78°C) flask containing phosphorus trichloride (1.5 ml, 17.0 mmol), under an atmosphere of nitrogen. The above mixture was allowed to warm to room temperature and then stirred for an additional 2 h. The reaction mixture was treated with dry triethylamine (11.7 ml), followed by the addition of benzyl alcohol (3.7 ml, 17.1 mmol) and the resulting suspension was stirred overnight. The reaction mixture was partitioned between ethyl acetate (350 ml, containing a trace of triethylamine) and water (100 ml). The organic layer was separated and the aqueous layer further extracted with ethyl acetate (150 ml). The combined organic extracts were dried (Na_2SO_4) and then evaporated to dryness in vacuo. The crude product was purified by short column chromatography on silica gel using hexane/triethylamine (10:1), yielding the product (4.9 g, 83%) as a pale yellow oil, which was made up to a 1 M solution in dry DCM (dichloromethane) and then stored under an atmosphere of nitrogen at −40°C. ^{1}H-NMR (300 MHz; $CDCl_3$; δ/ppm) 1.21 (12H, d, $J = 7.4$ Hz, $2 \times CH_3CHCH_3$), 3.68 (2H, m, $CH(CH_3)_2$), 4.72 (4H, m, $P(OCH_2Ph)_2$), 7.2–7.4 (10H, m, $2 \times Ph$).

3.1.2. 1-O-(1,2-ditetradecanoyl-sn-glycer-3-yl-phenyl-phosphoryl)-2,3:5,6-di-O-isopropylidene-4-O-(di-O-benzyl)-phosphoryl-D-myo-inositol (3)

1-*O*-(1,2-Ditetradecanoyl-*sn*-glycer-3-yl-phenyl-phosphoryl)-2,3:5,6-di-*O*-iso-propylidene-D-myo-inositol (**2**) (0.607 g, 0.667 mmol) and 1H tetrazole (0.454 g, 6.49 mmol) were dissolved in dry DCM (45.5 ml), under an atmosphere of nitrogen. A solution of *N,N*-diisopropyl-di-*O*-benzyl-phosphoramidite in dry DCM (3.3 ml, 1 M) was added and the resulting solution stirred for 4 h. A solution of *m*-chloroperoxybenzoic acid (2.43 g, 50–60%) in DCM (12.1 ml) was added to the reaction mixture and the solution stirred for a further hour. The reaction mixture was partitioned between DCM (200 ml) and saturated sodium sulphite solution (50 ml). The organic layer was separated and washed with saturated sodium bicarbonate solution (50 ml). The organic layer was then dried (Na_2SO_4) and evaporated to dryness in vacuo. The residue was purified by chromatography on silica gel ('G' Merck 7731 type 60) using diethyl ether/hexane (3:1), yielding the product (**3**) (0.685 g, 88%) as a colourless glass and as a mixture of diastereoisomers due to the chiral phosphorus. Accurate mass M^+, $C_{63}H_{96}O_{16}P_2$ requires 1171.4056. Found M^+, 1171.4051. ^{1}H-NMR (400 MHz; $CDCl_3$; δ/ppm) 0.88 (6H, t, $J = 7.0$ Hz, $(CH_2)_{12}CH_3$), 1.25 (40H, brd s, $(CH_2)_{10}CH_3$), 1.33 (1.5H, s, CH_3C), 1.37 (1.5H, s, CH_3C), 1.40 (1.5H, s, CH_3C), 1.41 (1.5H, s, CH_3C), 1.43 (1.5H, s, CH_3C), 1.51 (1.5H, s, CH_3C), 1.53 (1.5H, s, CH_3C), 1.55–1.63 (5.5H, m, CH_3C and $CH_2CH_2CO_2$), 2.28 (4H, m, CH_2CO_2), 3.47 (1H, $2 \times$ dd, $J = 5.2$, 10.8 Hz, H_5), 4.09 (1H, m, H_6), 4.13 (1H, m, H_3), 4.16 (1H, $2 \times$ dd, $J = 5.8$, 12.1 Hz, CH_2OCO), 4.28–4.37 (3H, m, CH_2OCO and $CHCH_2OP$), 4.40 (0.5H, t, $J = 4.6$ Hz, H_2), 4.63 (0.5H, t, $J = 4.6$ Hz, H_2), 4.67 (1H, m, H_4), 4.79 (1H, $2 \times$ ddd, $J = 4.3$, 10.3, 13.3 Hz, H_1), 5.11 (4H, m, $PhCH_2OP$), 5.24 (1H, m, CH_2CHCH_2), 7.18 (1H, m, PhOP), 7.27–7.38 (14H, m, PhOP and $2 \times PhCH_2OP$). The assignment of these resonances

was checked by a two-dimensional 'COSY' NMR experiment.

3.1.3. Sodium 1-O-(1,2-ditetradecanoyl-sn-glycer-3-yl-phosphoryl)-4-O-phosphoryl-D-myo-inositol (1)

1-*O*-(1,2-Ditetradecanoyl-*sn*-glycer-3-yl-phenyl-phosphoryl)-2,3:5,6-di-*O*-iso-propylidene-4-*O*-(di-*O*-benzyl)-phosphoryl-D-myo-inositol (0.685 g, 0.585 mmol) (**3**) was dissolved in ethanol (68.7 ml) and ethyl acetate (12.2 ml). Platinum(IV) oxide (0.44 g) was added and the resulting mixture hydrogenolysed at 50 p.s.i. for 5 h. The catalyst was removed by filtration. Water (5 ml) was added, the mixture was then allowed to stand overnight at room temperature and then at 40°C for 4 h. The reaction mixture was concentrated by evaporation in vacuo to approximately half volume, and aqueous ammonia solution (conc.) (3 ml) was added. The precipitate was collected by centrifugation and redissolved in water (30 ml). The solution was passed down an Amberlite IRC-50 (Na^+ form) ion exchange column, which was then washed with water (30 ml). The combined eluants were evaporated to dryness in vacuo, yielding the product (290 mg, 55%) as a white solid which was shown by TLC on oxalate treated silica to be a mixture of two components. Separation of the mixture was achieved in two different ways. (1) The silica (HF_{254}) was slurried from a 1% potassium oxalate aqueous solution and then washed with distilled water (about 10 times). The silica was then dried at approximately 350°C for 24 h before use. The treated silica (25 g) was slurried in chloroform/methanol/ammonia (conc.) (9:7:2). A chromatography column was constructed and washed with chloroform:methanol (9:7). The above reaction mixture (90 mg) was dissolved in dilute ammonia solution and preadsorbed onto treated silica. The silica was then applied to the column, which was eluted with a gradient of chloroform: methanol/ammonia (conc.) 9:7:0.5 to 9:7:2. The more polar component was isolated and passed down an Amberlite IRC-50 (Na^+ form) ion exchange column, yielding the product (**1**) (60 mg, 66%) as a white solid. (2) Alternatively, the mixture was separated by reprecipitation. The reaction mixture (150 mg) was dissolved in a small volume of distilled water (so the solution was still viscous). Methanol was then added until precipitation was complete, and the precipitate was collected by centrifugation. The procedure was repeated until TLC showed only one spot. This eventually gave the pure product (**1**) (55 mg, 37%) as a white solid.

After either purification route, the material was dried rigorously by desiccation over P_2O_5, under high vacuum for 1 week. Elemental analysis showed the compound to be a tetrahydrate. $C_{37}H_{69}Na_3O_{16}P_2 \cdot 4H_2O$ requires: C, 45.6; H, 8.01; P, 6.37; Na 7.09. Found: C, 45.4; H, 7.8; P, 6.2; Na, 7.25%. ^{1}H-NMR (400 MHz; CD_3OD; δ/ppm) 0.86 (6H, t, $J = 7.0$ Hz, $(CH_2)_{12}\underline{CH_3}$), 1.29 (40H, brd s, $(\underline{CH_2})_{10}CH_3$), 1.59 (4H, m, $\underline{CH_2}CH_2CO_2$), 2.34 (4H, m, $\underline{CH_2}CO_2$), 3.42 (1H, t, $J = 10.2$ Hz, $\underline{H_5}$), 3.55 (1H, dd, $J = 2.5$, 9.5 Hz, $\underline{H_3}$), 3.84 (1H, t, $J = 9.8$ Hz, $\underline{H_6}$), 3.92 (1H, dt, $J = 2.5$, 8.1 Hz, $\underline{H_1}$), 4.08 (2H, m, $\underline{CH_2}OP$), 4.20 (2H, m, $\underline{H_2}$ and $CH_2\underline{CH}CH_2OP$), 4.24 (1H, q, $J = 8.1$ Hz, $\underline{H_4}$), 4.46 (1H, dd, $J = 3.0$, 9.0 Hz, $CH_2\underline{CH}CH_2OP$), 5.23 (1H, m, $CH_2\underline{CH}CH_2$).

3.1.4. [4(6)-^{2}H]Myo-inositol

The reaction of 4(6)-myo-inosose [16] was performed using sodium amalgum [17]. When the reaction was judged complete (by ^{1}H-NMR spectroscopy in D_2O), the mercury was decanted off and the mixture was evaporated to dryness in vacuo. The residue was redissolved in water (80 ml) and the solution passed down an Amberlite IR 120 (H^+) ion exchange column. The solution was then evaporated to dryness in vacuo. The mixture of epimers was separated by dissolving the residue in boiling water (3 to 4 parts), glacial acetic acid was then added until the solution remained cloudy when boiled. The solution was then allowed to cool overnight. Pure [4(6)-^{2}H]myo-inositol (4.98 g, 61%) was obtained, by filtration, as a white crystalline solid of m.p. 220–223°C. Elemental analysis $C_6H_{11}O_6D$ requires: C, 39.80; H/D, 7.22%. Found: C, 39.90%; H/D, 7.05%. Mass spectroscopy (EI) (m/z) 181 (M^+, 1%) 74 ($C_3H_4O_2D^+$, 100%) 61 ($C_2H_3O_2D^+$, 30%). ^{1}H-NMR (300 MHz; D_2O; δ/ppm) 3.17 (1H, pseudo d, $J = 9.4$ Hz, $\underline{H_5}$), 3.43 (2H, m, $\underline{H_1}$ and $\underline{H_3}$), 3.51 (1H, m, $\underline{H_4}$ and $\underline{H_6}$), 4.00 (1H, s, $\underline{H_2}$).

3.1.5. 1,2-O-isopropylidene-3-[^{2}H]-sn-glycerol

1,2-*O*-Isopropylidene-*sn*-glyceraldehyde (3.93 g, 30.3 mmol) dissolved in dry tetrahydrofuran (4 ml) was added dropwise to a cooled (0°C) suspension of

lithium aluminium deuteride (1 g, 23.8 mmol) in dry THF (4 ml), over a period of 20 min. The reaction mixture was allowed to warm to room temperature and was then stirred for an additional 1.5 h. Water was added dropwise until effervescence ceased, and the mixture was then partitioned between diethyl ether (200 ml) and water (50 ml). The organic layer was separated and the aqueous layer further extracted with diethyl ether (2×100 ml). The combined organic extracts were dried ($MgSO_4$) and then evaporated to dryness in vacuo. The crude product was purified by distillation, to yield product (2.73 g, 68%) as a colourless oil of b.p. 125–130°C/170 mmHg. ^{1}H-NMR (300 MHz; $CDCl_3$; δ/ppm) 1.37 (3H, s, CH_3C), 1.44 (3H, s, CH_3C), 2.78 (1H, brd s, OH), 3.58 (0.5H, brd s, CHDOH), 3.69 (0.5H, brd s, CHDOH), 3.78 (1H, dd, $J = 7.4$, 8.3 Hz, CHOC), 4.05 (1H, pseudo t, $J = 7.4$ Hz, CH_2OC), 4.23 (1H, pseudo q, $J = 5.5$ Hz, CH_2OC).

3.2. Instrumental and analytical methods

3.2.1. X-ray diffraction

Preliminary diffraction experiments were performed using X-rays generated by a Marconi–Elliot GX13 rotating anode instrument with point collimation and a 175 mm path length. These experiments were performed to ensure that the DMPI-4P/DMPC 50:50 (molar ratio) mixtures used in these studies at 25°C was in the L_α phase and were homogeneous. A 50:50 (molar ratio) mixture of DMPC/DMPI-4P was prepared on a quartz glass, arched plate ($\sim$ 3 mg total lipid), as described below for the neutron diffraction experiments. Under these conditions, at 25°C, the DMPI-4P/DMPC samples were shown to be in the L_α phase and homogeneous The picture showed discrete Bragg reflections which could be simply indexed to a lamellar unit cell. Only one series of Bragg peaks was observed and no off-axis peaks were seen.

3.2.2. Neutron diffraction

A solution of DMPC in methanol was sonicated, as was a solution of DMPI-4P in H_2O. The two solutions were mixed together to provide a solution of 50:50 (molar ratio) DMPC/DMPI-4P, 20 mg total lipid. The solution was applied to a flat quartz slide (50×20 mm) using an artists' air-brush, utilising oxygen-free nitrogen as a propellent. The resulting sample was dried under high vacuum for at least 8 h prior to use. The dried sample was rehydrated in a 98% humid atmosphere, using H_2O, D_2O or a mixture of the two, and allowed to reach equilibrium over a period of at least six hours. The sample was transferred rapidly to the sample holder goniometer of the membrane diffractometer, H3B, at the HFBR, Brookhaven National Laboratory, Long Island, New York, U.S.A., where it was then sealed hermetically in a 98% humid atmosphere of 0% D_2O, 33.3% D_2O, 66.6% D_2O or 100% D_2O (by volume). The sample was allowed to equilibrate for at least half an hour prior to data collection. Diffraction data were collected using neutrons of wavelength 2.07 Å and beam dimensions of 20 (vertically) $\times$ 1 (horizontally) mm. The data were collected in the form of 19 files for each order of diffraction, representing a range of $-0.45°$ to $+0.45°$ from the centre of the angle that gave maximal diffracted intensity for that order. Six orders of diffraction ($\sim$ 8 h exposure time) were collected for each sample at each composition of H_2O/D_2O. After the scan was complete the sample was removed, dehydrated and then rehydrated under the next H_2O/D_2O mixture. Each sample was checked to ensure that the maximal diffraction occurred at the same positions as before, any sample failing this check was discarded.

3.3. Analysis of the hydration level

The hydration levels of the samples prepared in this manner were determined by radiochemical double labelling experiments. The mixture was prepared as described above, and a small (ng) quantity of ^{14}C-labelled DPPC (Amersham) was added. The samples were placed on small glass plates, and the sample was dried under high vacuum. The plates were hydrated under an atmosphere containing a known quantity of ^3H_2O (Amersham) over a period of 8 h at 25°C. The plates were then immediately transferred to tubes containing scintillation fluid. The radioactivity of both ^{14}C and ^{3}H were measured for each sample, the standard and a sample of the $^3H_2O/H_2O$ mixture. After compensating for cross-talk between the two channels, the number of moles of sample and H_2O on each slide was determined, using the standards, the ratio between the two was calculated to

give the hydration ratio. For the DMPI-4P/DMPC samples this hydration ratio (waters per lipid molecule was found to be 27 ± 4 (average of 8 independent measurements).

3.4. Data analysis

The two-dimensional data from the H3B detector were collapsed into a one-dimensional (horizontal) spectrum by summing the channels vertically. The Bragg peaks were isolated from the background and integrated using a commercial program, Sigmaplot (Jandel Scientific, Corte Madera, Ca, USA). A Gaussian distribution was fitted to each diffraction peak after subtraction of the background by least-squares line fitting to the area immediately surrounding the peak. Each Bragg peak had been recorded by scanning the sample through a narrow range (-0.45 to $+0.45°$, 19 files) centred on the Bragg angle. For the highest orders of diffraction this scan was not always wide enough to record the whole of the peak. To correct for this, the data were replotted as intensity against sample angle. Gaussian-fitting was again carried out to enable the total integral, including those parts of the Gaussian outside the scan range, to be calculated. A number of corrections were applied to the integrated intensities, as described previously [20,21]. Each sample had been run at four different concentrations of D_2O in H_2O (0, 33, 66 and 100%). It has been shown [22] that the scattering density of the region between the bilayers (representing the H_2O or D_2O) progressively increases with increasing D_2O concentration. In general, the amplitudes of the even order reflections will increase, whilst negative orders will decrease, though this relationship breaks down at higher orders of diffraction (see Fig. 1). The data sets may therefore be both phased and scaled to each other by simultaneously applying this straight-line relationship to all orders. A further constraint on the line-fitting comes from the observation that if the water distribution is the same for any data sets, for example, the different deuterated analogues of DMPI-4P in the DMPI-4P/DMPC sample, then the gradient of the lines fitted to the same order of diffraction will also be the same. Subsequent to this four-point method, a variation on the isomorphous replacement technique was employed, where the peaks corresponding to deuterium labels on the lipid itself were used as end-points in Fourier subtractions and phases were assigned in order to obtain such profiles. Excellent agreement was achieved between these complimentary phasing approaches. The diffraction data were placed on a 'relative absolute' scale using the procedure developed by White and his co-workers [23,24], whereby, known differences in mean scattering density caused by the introduction of other molecules, or by the selective replacement of hydrogen by deuterium, are used to scale the data sets absolutely with respect to the unit cell contents. By this method the relative scaling of each pair of data sets is adjusted until the area under their difference

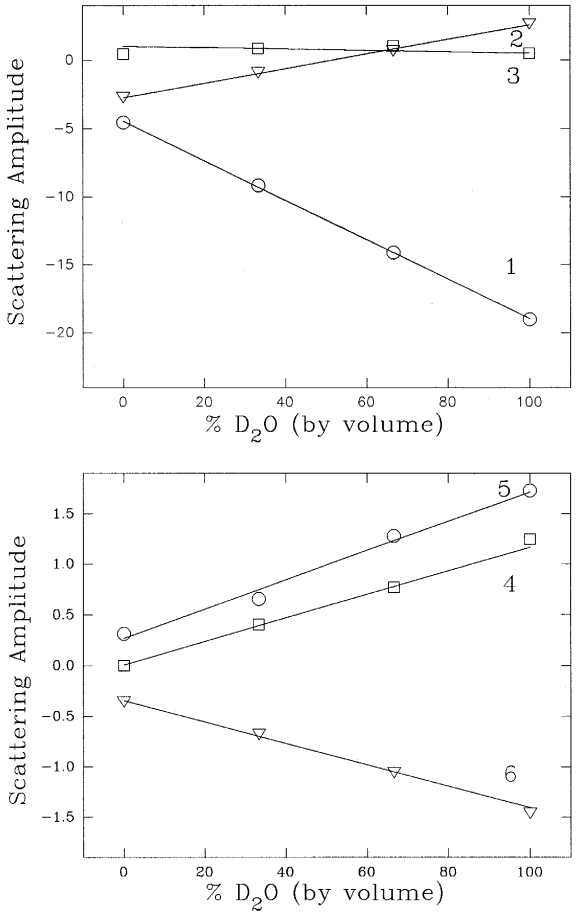

Fig. 1. A plot of neutron scattering amplitude vs. D_2O concentration. A straight line may be fitted to each order as the difference between two points is just dependent upon the D_2O distribution and not the sample. Note that the slopes for the 5th and 6th orders are opposite to those for the other odd and even orders, respectively. This is a consequence of the inability to describe the D_2O distribution by a single Gaussian [23,8].

Table 1
Structural factors for DMPC-4P/DMPC (50:50 molar ratio) system at 0% D_2O on a 'relative absolute' scale (± 0.08) for all of the samples studied

Sample	Order 1	Order 2	Order 3	Order 4	Order 5	Order 6
d_0	−3.621	−0.847	+1.121	+0.133	+0.263	−0.336
$d_{4,6}$	−4.082	−1.084	+1.447	0.000	+0.278	−0.399
d_2	−4.321	−1.977	+1.472	0.000	+0.431	−0.417
$d_{sn\text{-}3}$	−4.456	−2.760	+1.022	+0.007	+0.269	−0.345
d_{1-6}	−10.380	−3.457	+3.253	−0.503	+0.597	−0.236

transform is equal to the difference in their total scattering lengths (per unit cell), and the area under the transform of each set is equal to the total scattering length for the unit cell contents. The neutron data were scaled using the known scattering densities of D, H_2O and D_2O. The structure factors for all the of the various deuterated analogues are tabulated on a relative scale in Table 1. The neutron diffraction scattering profiles were determined by Fourier transform (essentially the summation of the cosine curves multiplied by their structure factor for each order of diffraction). Typical scaled profiles of the DMPI-4P/DMPC system is shown in Fig. 2, displaying the $d_{sn\text{-}3}$ DMPI-4P/DMPC profile, the d_0 DMPI-4P/DMPC profile and the subtracted profile representing the site of deuteration. This process may be carried out in real space or reciprocal space. When the latter approach is used with a variety of D_2O concentrations, any differences in the result can be used as an estimate of the error in the data points. The errors quoted in Table 1 represent the maximum observed error, when this estimation was carried out for each individual structure factor, over all possible subtractions. In order to determine the accurate position of the centre of the neutron scattering density associated with the site of deuteration Gaussian fitting to the subtracted profile was performed. The Gaussian fitting was performed by minimising the sum of the absolute errors of the orders of diffraction using the following equation:

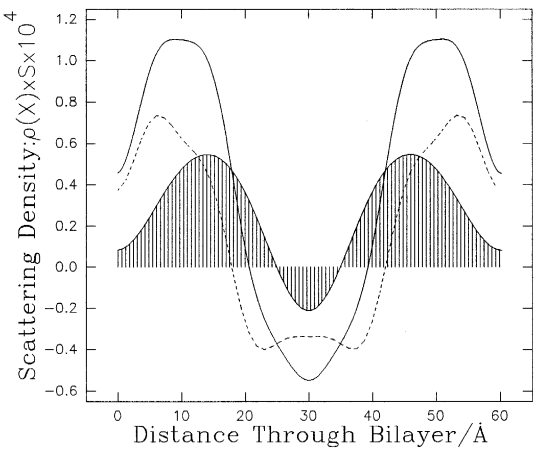

Fig. 2. The neutron scattering density profiles for samples of DMPI-4P/DMPC (50:50 molar ratio system) using six orders of diffraction plotted on a 'relative absolute' scale. The water of the bilayer is represented at the extremes of the profiles. The profiles shown are those of the DMPI-4P ($d_{sn\text{-}3}$) material (continuous line), the DMPI-4P (d_0) material (dashed line) and the difference between the two profiles, i.e., the distribution of the deuterium label (hatched area).

$$A_{\mathrm{Err}} = \frac{\Sigma|[F_{\mathrm{Obs}}(n) - F_{\mathrm{Calc}}(n)]|}{\Sigma|[F_{\mathrm{Obs}}(n)]|}$$

where $F(n)$ is the structure factor for order number, n. Hence, the position of the d_2 label was determined by subtracting the d_0 DMPI-4P/DMPC profile from the d_2 DMPI-4P/DMPC profile, and subsequent Gaussian fitting to the resulting profile. Similarly, for the $d_{sn\text{-}3}$ DMPI-4P/DMPC sample, the Gaussian parameters were used to determine the centre of neutron scattering density representing the site of deuteration. For the $d_{4,6}$ DMPI-4P/DMPC sample, the d_0 DMPI-4P/DMPC sample was subtracted as before, and two Gaussian curves were fitted to the subsequent profile with a resulting smaller error than when a single Gaussian was fitted to the subtracted profile. For the d_6 material, three Gaussian curves were fitted to the profile represented by $[(d_{1-6}-d_0)-2(d_{4,6}-d_0)-(d_2-d_0)]$. The Gaussian fitting was performed in reciprocal space to prevent errors from Fourier rippling. The results from the Gaussian fit-

Table 2
The distance from the centre of the site of deuteration to the reference planes – the centre of the hydrocarbon region ($l_{vert.}$) and to a plane parallel to this but passing through the glycerol *sn*-3 position

Position of deuterium label	Sample/data set	'Perpendicular' distance from the site of deuteration to the reference plane for the DMPI-4P/DMPC (50:50) system (±0.5 Å)	
		To the centre of the hydrocarbon region ($l_{vert.}$)	To a plane through the *sn*-3 carbon
Inositol ring position 1	d_{1-6}–d_2–$d_{4,6}$	20.8 (8)	4.1 (8)
Inositol ring position 3	d_{1-6}–d_2–$d_{4,6}$	21.8 (8)	5.1 (8)
Inositol ring position 5	d_{1-6}–d_2–$d_{4,6}$	23.1 (9)	6.4 (9)
Inositol ring position 4	$d_{4,6}$	20.8 (8)	4.1 (8)
Inositol ring position 6	$d_{4,6}$	21.1 (8)	4.4 (8)
Inositol ring position 2	d_2	18.8 (8)	2.1 (8)
Glycerol *sn*-3 position	$d_{sn\text{-}3}$	16.7 (0)	–

Values refer to maximum of the fitted Gaussians (see text).

ting, in terms of the vertical distance from the site of deuteration to the centre of the bilayer ($l_{vert.}$) and also the *sn*-3 position, are shown in Table 2. The distances tabulated in Table 2 were used for the subsequent molecular modelling calculations.

3.5. Modelling of the inositol ring orientation and headgroup conformation

In order to determine the orientation of the inositol ring, on the basis of the data in Table 2, calculations were performed using the COSMIC (COmputational and Structure Manipulation in Chemistry) [30] program. A subroutine was written within COSMIC, which calculated the vertical distance between all fifteen pairs of protons on the inositol ring (i.e., the distance parallel to the bilayer normal between H_1 and H_2, H_1 and H_3, H_1 and H_4 etc.) as a function of the ring orientation. The absolute difference between the calculated value and the corresponding experimentally determined value (from Table 2) for each of the pairs of inositol protons was calculated, and the total RMS error determined. The full orientational space for the inositol ring was generated making the a priori assumption that the P/ODAG bond was parallel to the bilayer normal. The choice of this method for generating the orientational space for the ring makes comparison with previous studies [5,6] somewhat easier and allows it to be related to two internal conformational variables, the dihedral angles α_1 and α_2 (Fig. 3A), which, in turn, relate in a simple manner to models for intramolecular hydrogen bonding [5]. It should be noted, however, that the derived orientation of the ring relative to the bilayer normal is only dependent on the value of $l_{vert.}$ for each deuterium and any model that generates the full orientational space would have served equally well. Using this approach the RMS error of the fit can be displayed as a function of α_1 and α_2 as shown in Fig. 3B. Since the ring can be treated as a rigid entity

Table 3
The effect of changing the assignment of the deuteriums between positions 3, 4, 5 and 6 on the error for the best possible fit to the data

Assignment (distance to the centre of the hydrocarbon region $l_{vert.}$, Å)						Best fit per constraint (Å)
H_1	H_2	H_3	H_4	H_5	H_6	
20.88	18.88	21.88	20.88	23.19	21.18	0.03
20.88	18.88	21.88	21.18	23.19	20.88	0.04
20.88	18.88	23.19	20.88	21.88	21.18	0.40

The errors are expressed as per H–H distance constraint. Exchanging the assignment for positions 4 and 6 has almost no effect on the calculated best orientation of the ring or the quality of the fit. Permutations in the assignments for positions 1, 3 and 5 all result in much poorer fits. The 'least bad' of the options being the exchange of the assignments for positions 3 and 5 (shown).

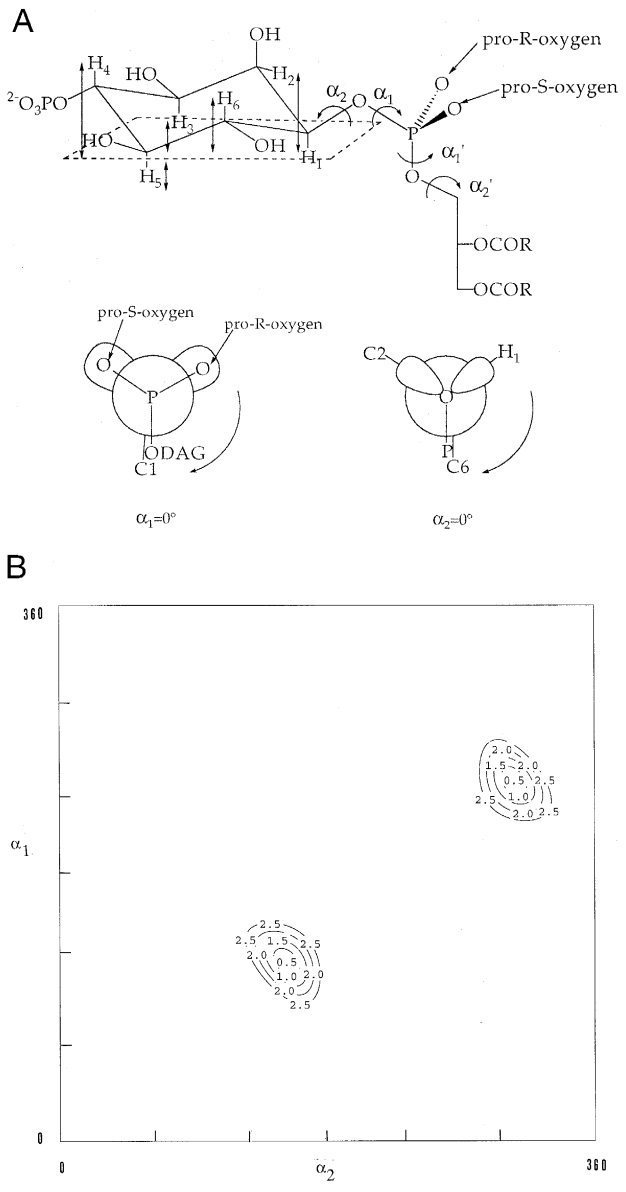

Fig. 3. A: the dihedral angles that determine the orientation of the headgroup portion of the molecule, and 5 of the 15 distance constraint measurements (the distances from H_2–H_6 to a plane through H_1 and measured parallel to the membrane normal) used to compare the experimentally determined values to those generated by the computer model. B: the contour map generated by molecular modelling calculations (see text). The error contours represent the total (over fifteen constraints or fifteen H–H distances) of the RMS errors. The map shown only displays values for α_1 and α_2 for which the sum of the total errors was less than 3 Å. The values for the dihedral angles at the error minima were used to construct the orientational and conformational diagram shown in Figs. 4 and 5.

$l_{vert.}$ for three of the hydrogens would provide the minimum data to fix the ring orientation. Specific deuteration of three single sites would be a very difficult task, but the neutron diffraction studies on these mono- and polydeuterated systems provided equivalent information. It provided a direct measure for $l_{vert.}$ for the hydrogen H_2, of $l_{vert.}$ for a pair of hydrogens corresponding to those at H_4 and H_6 and of $l_{vert.}$ for the three hydrogens corresponding to those at positions H_1, H_3, and H_5 (by subtraction of the data for the d_2 and $d_{4,6}$ systems from that for the d_{1-6} system). To solve this, both assignments of H_4 and H_6 and all six possible assignments for the hydrogens H_1, H_3, and H_5 were studied. Only three possible ways of assigning the hydrogens gave reasonable assignments to the experimental data and these are given in Table 3 along with the minimum error per single H–H distance for each of the various assignments. The assignment corresponding to the best fit was as shown in Table 2. As can seen from Table 3, almost as good a fit was obtained when the assignments for the 4 and 6 positions were reversed, and a reasonable fit of assignments when the 3 and 5 positions reversed. Other combinations proved much worse. In fact, reversing assignments 4 and 6 or 3 and 5 makes virtually no difference to the predicted orientation of the ring.

4. Discussion

The conformational behaviour of many of the commoner phospholipids has been reviewed elsewhere [25,26]. Studies of phosphatidylcholine [27], phosphatidylethanolamine [28] and phosphatidylglycerol [29] all suggest that the headgroups lie approximately flat on the surface of the membrane. A simplifying factor for the phosphoinositides relative to these other lipids is that the cyclohexyl ring will adopt a single rigid chair conformation. The neutron diffraction data allows the orientation of this rigid unit and its depth within the membrane to be determined. The conformational problem relating to the ‘flexible’ parts of the headgroup is more difficult to solve and the neutron diffraction studies provide no information regarding the 4-phosphate or 2,3,5 and 6-hydroxyl groups. However, the assumption that the P/ODAG bond is perpendicular to the membrane (an assump-

tion justified in part from results for other lipids [31] and in part from the present study) allows reasonable models to be proposed for this portion of the system. Throughout, we have made the important simplifying assumption that the phosphoinositide headgroup exists in a single conformation and a single orientation.

4.1. Ring orientation

The contour map shown in Fig. 3B displays two distinct error minima, of more-or-less identical value. In order to determine the relationship between these two minima the corresponding three-dimensional images were superimposed. The results are shown in Fig. 4. It is apparent that these two minima correspond to a single best orientation of the inositol ring relative to the membrane. This is a tilted orientation in which the hydroxy group at C_5 points out into the aqueous layer.

4.2. Conformation of the portion of the headgroup connecting the diacylglycerol to the inositol ring

The only difference between the two minima shown in Fig. 4 is conformational – the value of the dihedral angles mapping back to the phosphate group and producing a P/ODAG bond orientation which is parallel to the bilayer normal. If it is assumed that this orientation of the P/ODAG bond is correct then, arising from the depth and fixed orientation of the inositol ring, there are two possible conformations for the portion of the headgroup connecting the diacylglycerol to the inositol ring. A stereoview of both conformations is shown in Fig. 5. In this figure the dihedral angles about the hydroxy and the 4-phosphate groups have been more-or-less arbitrarily chosen to maximise intramolecular hydrogen bonding interactions. The two possible/putative conformers are discussed in turn below.

4.2.1. Putative conformer A

In the putative conformer A (Fig. 5A) $\alpha_1 = 119°$ and $\alpha_2 = 153°$. With this conformation there are no obvious intramolecular hydrogen bonding possibilities except a possible long-range intramolecular hydrogen bond between the C6-hydroxyl group and the pro-*R*-oxygen of the phosphate. This oxygen–oxygen distance was measured as 3.50 Å. There appears to

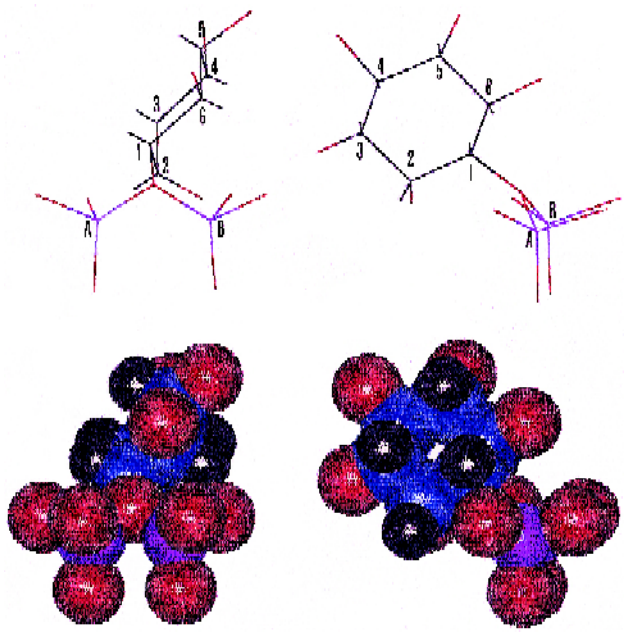

Fig. 4. Two views of a computer-generated image in which, for the two minima shown in Fig. 3, the orientation of the ring relative to the membrane has been maintained, and the six carbon atoms of the inositol ring (labelled 1–6) superimposed. Both involve the same orientation of the inositol ring and the different dihedral angles, α_1 and α_2, simply represent two mappings back to the phosphate group. For these, the phosphorus atoms are labelled A and B and these correspond to the putative conformations A and B shown in Fig. 5. Both mappings result in an alignment of the P/ODAG bond. parallel to the bilayer normal which, in this diagram is vertical with the outer surface, which is exposed to water, at the top. For the sake of clarity, the hydroxyl hydrogens and the 4-phosphate group have been omitted. Note that this orientation results in the hydrogen at C5 being uppermost, that at C2 closest to the centre of the membrane, and the four hydrogens at C1, C3, C4, C6 being at about the same intermediate 'depth' (cf. Tables 2 and 3).

be one atom–atom close contact. The axial-H_1 is within the Van der Waals contact distance of the pro-*S*-oxygen of the phosphate. This distance was measured as 2.37 Å, compared with the permissible minimum contact distance of 2.60 Å. The C2-hydroxyl group is in a position to hydrogen bond (intermolecularly) to the phosphate of a neighbouring molecule. The C3-hydroxyl group is similarly in a position to hydrogen bond intermolecularly with the phosphate of a neighbouring molecule, or alternatively, intramolecularly with the negatively charged 4-phosphate. The negatively charged 4-phosphate is in an orientation available for favourable electrostatic

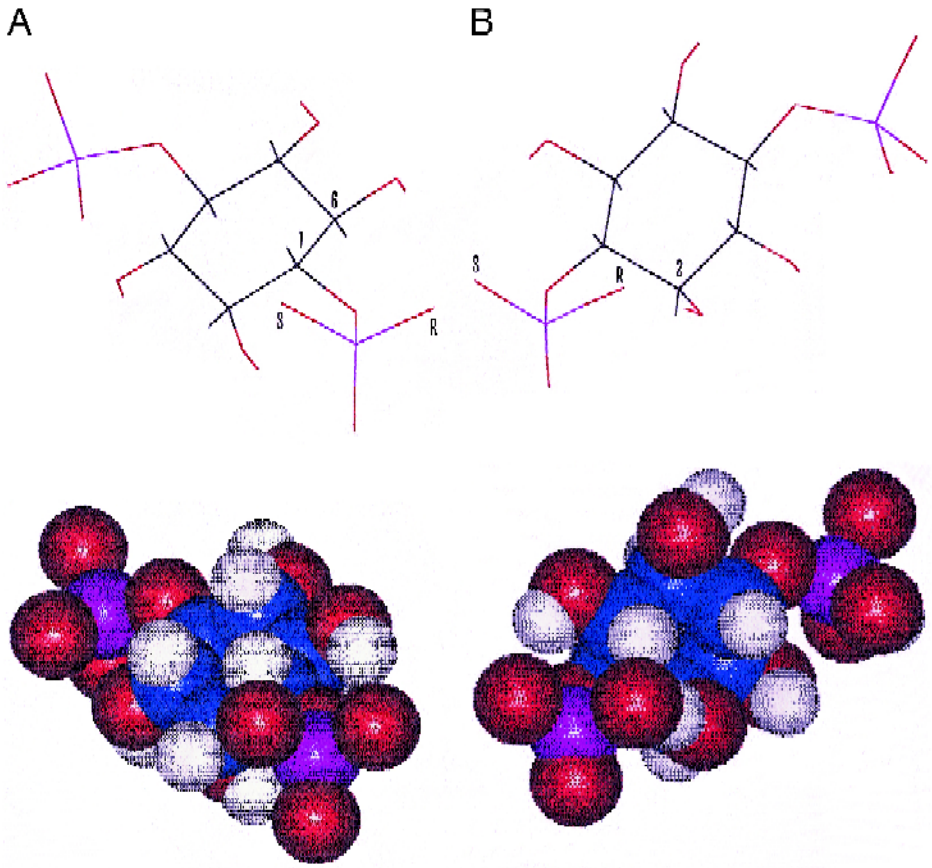

Fig. 5. The two putative conformations obtained from the computer modelling and discussed in the text. These are shown with the bilayer normal parallel to the vertical of the page, and shown so that the pro-*S*-oxygen of the phosphate diester (labelled S) is on the left the pro-*R*-oxygen of the phosphate diester (labelled R) is on the right. The dihedral angles for the carbon oxygen bonds C2–C6 are unknown but those at positions C2 and C6 have been adjusted to allow for intramolecular hydrogen bonding to the phosphate oxygens [5]. Putative conformer A has $\alpha_1 = 119°$ and $\alpha_2 = 153°$. There is the potential for a (rather long) hydrogen bond from the hydroxy group on C6 (labelled 6) and the pro-*R*-oxygen and a possible steric clash between the pro-*S*-oxygen and the hydrogen on C1 (labelled 1). The putative conformer B has $\alpha_1 = 241°$ and $\alpha_2 = 305°$. There is the potential for a hydrogen bond from the hydroxy group on C2 (labelled 2) and the pro-*R*-oxygen but the distance between these centres is very short and it is perhaps more realistic to visualise a steric clash between them. In either case, a slight adjustment of the dihedral angles removes the steric clash and improves the hydrogen bonding potential of the system.

interactions with neighbouring positively charged choline groups. The C5-hydroxyl group is free to hydrogen bond intermolecularly with the aqueous media.

4.2.2. Putative conformer B

In the putative conformer B (Fig. 5B), the conformation corresponds to $\alpha_1 = 241°$ and $\alpha_2 = 306°$. This arrangement allows a potentially strong intramolecular hydrogen bond between the axial C2-hydroxyl group and the pro-*R*-oxygen of the phosphate. However, the oxygen–oxygen distance between the C2-hydroxyl group and the pro-*R*-oxygen is within the Van der Waals contact distance. This distance was measured as 2.04 Å, compared with the allowable distance of 2.80 Å. There is a second atom–atom close contact interaction, which is between the axial-H_6 and the pro-*R*-oxygen. This distance is 1.99 Å, compared with the allowable value of 2.60 Å. The C3-hydroxyl group is in a position to intermolecularly hydrogen bond with the phosphate of a neighbouring molecule, or alternatively, intramolecularly with the 4-phosphate group. The negatively charged 4-phosphate group is in a position to interact with a

neighbouring positively charged choline group. The C5- and C6-hydroxyl groups are free to intermolecularly hydrogen bond with the aqueous media.

A choice between the putative conformers A and B is not easy. Conformer A has no potential intramolecular hydrogen-bonding patterns to the phosphodiester, but neither are there any strong atom–atom repulsive interactions. Conformer B, on the contrary, has a strong intramolecular hydrogen-bond between the C2-hydroxyl group and the pro-*S*-oxygen of the phosphate, but also unreasonably close atom–atom interactions. Given that, in other lipids, *inter*-molecular H-bonding is favoured, the absence of a strong *intra*-molecular H-bond in conformer A is probably unimportant and, given that this also lacks the unacceptably close atom–atom contacts found in conformer B, it is probably favoured.

4.3. Analysis of the data for the sn-3 position

Underlying the extrapolation from the determined orientation of the inositol ring to the putative conformers A and B was the assumption that the P/ODAG bond is parallel to the bilayer normal. If this is not strictly true, but it is slightly tilted, then for putative conformer B it is possible that the C2-hydroxyl oxygen and pro-*S*-oxygen distance will increase to outside the Van der Waals interaction distance, but still allow intramolecular hydrogen-bonding. We hoped that we could use $l_{\text{vert.}}$ for the ring deuteriums relative to the deuterium at the glycerol *sn*-3 position (Table 2) to test this hypothesis. Firstly, it was essential to demonstrate that $l_{\text{vert.}}$ for the *sn*-3 hydrogen is consistent with the conformations shown in Fig. 5 and this was readily achieved. Using the two conformations described above, the error per inositol proton to the *sn*-3 proton (vertical distance) was calculated as a function of the dihedral angle about the O–$C_{sn\text{-}3}$ bond. (Note that these calculations of $l_{\text{vert.}}$ are unaffected by rotation about the P/ODAG bond, hence, only rotation about the O–$C_{sn\text{-}3}$ bond needs to be considered.) The results are summarised in Fig. 6. It is apparent that the $d_{sn\text{-}3}$ results are consistent with either of the putative conformations, and it suggests that the favoured value of this dihedral angle is *trans*. Note also that there is little difference between the two conformations, but conformer B fits the data slightly better. Secondly, it was

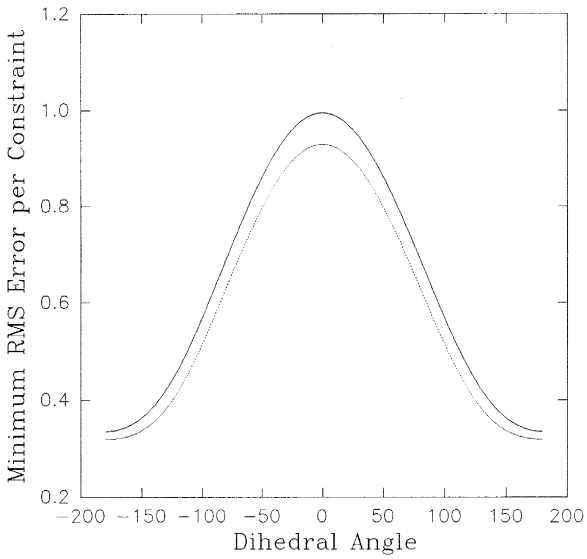

Fig. 6. A graph to show the variation in the error of the computer modelling fit with the experimental data with the dihedral angle α_2'. The solid line represents conformer A and the dotted line conformer B. Note that the best fit is obtained with this bond approximately *trans*.

hoped to use the $d_{sn\text{-}3}$ data to *prove* the parallel arrangement of the P/ODAG bond to the bilayer normal. This was unsuccessful. In order to test the fitting of the data when the orientation of the P/ODAG bond is allowed to vary, further molecular modelling calculations were performed with the inositol ring fixed in the correct orientation and at the correct distance from the centre of the membrane. All the dihedral angles α_1, α_2, α_1' and α_2' were varied, the minimum error in the depth of the *sn*-3 deuterium for each orientation of the P/ODAG bond relative to the bilayer normal was calculated and recorded, as was the $C_{sn\text{-}3}$–$C_{sn\text{-}2}$ bond orientation (relative to the bilayer normal), the four values for the dihedral angles and the minimum error. The minimum error plotted as a function of the angle of the P/ODAG bond to the bilayer normal is shown in Fig. 7. as may be seen, the *sn*-3 data can be fitted over a large range ($\sim$ 0–80°) of the orientation of the P/ODAG bond to the bilayer normal. A large part of this range is obviously impractical in natural membranes, as a P/ODAG bond at 80° to the bilayer normal would bury the negatively charged phosphate oxygens in the hydrophobic part of the membrane. The wide range of values is a consequence of the flexibility in the

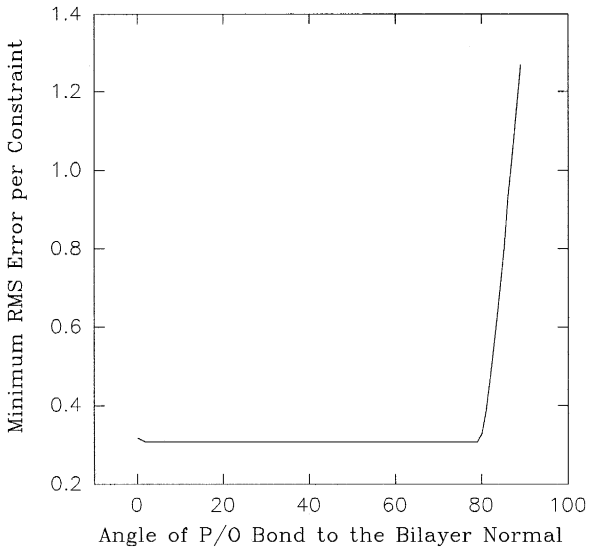

Fig. 7. A plot to show the variation in the error of the computer modelling fit to the experimental data as a function of the angle between the P/ODAG bond and the bilayer normal. Note that 0° implies that O–P is in the same direction as the bilayer normal and that the data can be fitted equally well up to a situation in which the bond is tilted at an angle of 80°.

system where there is four free dihedral angle variables. However, it became apparent during the calculation that the values of α_2' for all error minima (i.e., at all minima values of the orientation of the P/ODAG bond to the bilayer normal) were identical, 176.2°. This value is consistent with the *trans* orientation described in Fig. 6, and also X-ray data of other phospholipids, where, for example, in the two crystalline conformations of DMPC this dihedral angle was measured as 163 and 177° [32]. This suggests that there should be an approximately parallel alignment of the P/ODAG and $C_{sn\text{-}3}$–$C_{sn\text{-}2}$ bonds, for all orientations of the P/ODAG bond to the bilayer normal. A plot of the P/ODAG bond orientation vs. the $C_{sn\text{-}3}$–$C_{sn\text{-}2}$ bond orientation should give approximately a straight line, this plot is shown in Fig. 8, which displays an approximately linear relationship, within the range of values over which the data could be fitted.

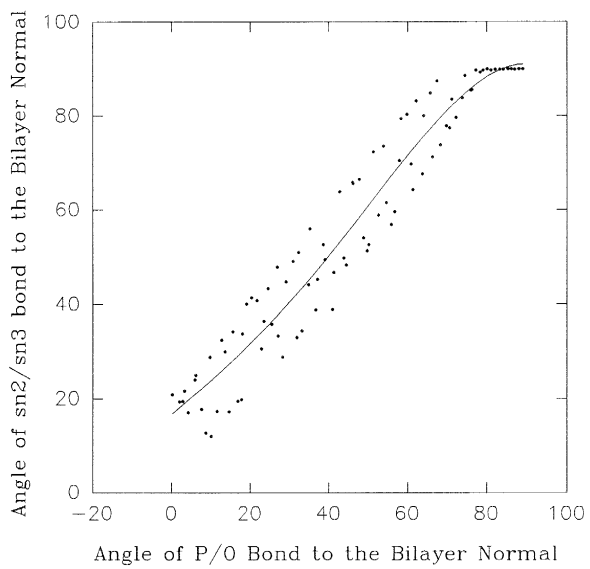

Fig. 8. A plot of 'best fit' data for the orientation of the $C_{sn\text{-}3}$—$C_{sn\text{-}2}$ bond as a function of the orientation of the P/ODAG bond. A regression best-fit line has been applied to the data points.

5. Conclusions

Whereas attempts to determine the headgroup orientation of inositol lipids by ^{1}H- and ^{2}H-NMR had failed to give a definitive answer, neutron diffraction experiments on specifically deuterated lipids have allowed the determination of $l_{\text{vert.}}$ (the vertical distance to the centre of the bilayer) for each hydrogen in the inositol ring to approximately ± 0.5 Å. This data, in conjunction with computer modelling has suggested a single tilted orientation (Figs. 4 and 5) of the inositol ring of DMPI-4P in a model membrane in the L_α phase, i.e., a 1:1 molar mixture of DMPI-4P with dimyristoyl-phosphatidylcholine hydrated to the level of 28 water molecules per lipid molecule. The reason for this orientation is unclear, but is probably associated with electrostatic attraction between the negatively charged 4-phosphate group and the positive pole of the trimethylammonium group of the DMPC, which is known to lie close to the membrane surface [27]. In this sense, it can be argued that the result is probably significant for the environment within natural biomembranes since PI-4P is normally present in an environment in which PC and PE are the dominant lipid components. In this orientation, the C5 hydroxyl group is extended into the aqueous phase, and it is therefore the most accessible to water borne species. This result may be significant in that it is the 5-position of the inositol ring which is phosphorylated in the PI to PI-4P to PI-4,5P_2 sequence.

Although the ring orientation and its position within the membrane (its distance from the centre) have been unambiguously assigned, the conformation/orientation of the $O(PO_2)O$ portion of the headgroup connecting the diacylglycerol to the inositol ring. is still unclear. Molecular modelling has shown that, if we make the common assumption that the P/ODAG bond is parallel to the bilayer normal, then there are two possible mappings from the ring to the phosphate group. Selective distinction between these two is difficult. One conformation (conformation B) has an atom–atom close contact occurring between the oxygen of the C2 hydroxyl group and the pro-*R*-oxygen of the phosphate, for this reason it is suggested that conformer A is favoured. However, for either of these conformations, a small deviation from the P/ODAG bond being parallel to the bilayer normal arrangement may remove the close atom–atom interactions. In order to test the hypothesis of a parallel alignment of the P/ODAG bond to the bilayer normal further molecular modelling calculations were performed incorporating data for $l_{vert.}$ for the hydrogens in the inositol ring and for the *sn*-3 position of the glyceryl reside. Unfortunately, due to the flexibility inherent in a system where four dihedral angles may be varied freely, a broad range of solutions to the orientation of the P/ODAG bond to the bilayer normal was shown to fit the data. However, this modelling work did show that the best fit is always attained when the dihedral angle α_2' (about the *sn*-3 carbon to phosphate oxygen bond Fig. 3) is approximately *trans*.

Acknowledgements

The authors wish to thank the EPSRC (SERC) for financial assistance and the Department of Energy, USA, for use of facilities.

References

[1] J.P. Bradshaw, R.J. Bushby, C.C.D. Giles, M.R. Saunders, D.G. Reid, Preliminary communication of part of this work, Nature Struct. Biol. 3 (1966) 125–127.
[2] M.J. Berridge, Annu. Rev. Biochem. 56 (1987) 159–193.
[3] A.R. Saltiel, Diabetes Care 13 (1990) 244–256.
[4] M.G. Low, Biochim. Biophys. Acta 988 (1989) 427–454.
[5] R.J. Bushby, S.J. Byard, P.M. Hansbro, D.G. Reid, Biochim. Biophys. Acta 1044 (1990) 231–236.
[6] P.M. Hansbro, S.J. Byard, R.J. Bushby, P.J.H. Turnbull, N. Boden, M.R. Saunders, R. Novelli, D.G. Reid, Biochim. Biophys. Acta 1112 (1992) 187–196.
[7] G. Büldt, H.U. Gally, A. Seelig, J. Seelig, G.J. Zaccai, Nature 271 (1978) 182–184.
[8] J.P. Bradshaw, C.E. Dempsey, A. Watts, Mol. Membr. Biol. 11 (1994) 79–86.
[9] R.C. Young, C.P. Downes, D.S. Eggleston, M. Jones, C.H. MacPhee, K.K. Rana, J.G. Ward, J. Med. Chem. 33 (1990) 641–646.
[10] M. Jones, K.K. Rana, J.G. Ward, R.C. Young, Tetrahedron Lett. 30 (1989) 5353–5356.
[11] K.-L. Yu, B. Fraser-Reid, Tetrahedron Lett. 29 (1988) 979–982.
[12] E. Uhlmann, J. Engels, Tetrahedron Lett. 27 (1986) 1023–1026.
[13] T. Tanaka, S. Tamatsukuri, M. Ikehara, Tetrahedron Lett. 27 (1986) 199–202.
[14] F. Gonzalez-Sastre, F. Folch-Pi, J. Lipid Res. 9 (1968) 532–533.
[15] T. Shibata, J. Uzawa, Y. Sugiura, K. Hayashi, T. Takizawa, Chem. Phys. Lipids 34 (1984) 107–113.
[16] T. Posternak, Biochem. Prep. 2 (1952) 57–64.
[17] T. Posternak, W.H. Schopfer, D. Reymond, C. Lark, Helv. Chim. Acta 41 (1958) 235.
[18] C.C.D. Giles, Thesis, Leeds, 1995.
[19] D.Y. Jackson, Synth. Commun. 18 (1988) 337–341.
[20] K.C. Duff, A. Cudmore, J.P. Bradshaw, Biochim. Biophys. Acta 1145 (1993) 149–156.
[21] K.C. Duff, P.J. Gilchrist, A.M. Saxena, J. P Bradshaw, Virology 202 (1994) 287–293.
[22] W.P. Franks, W.R. Lieb, in: G.C. Knight (Ed.), Liposomes: From Physical Structure to Therapeutic Applications, Elsevier, Amsterdam, 1981, pp. 243–272.
[23] M.C. Weiner, G.I. King, S.H. White, Biophys. J. 60 (1991) 568–576.
[24] R.S. Jacobs, S.H. White, Biochemistry 28 (1989) 3421–3437.
[25] H. Hauser, I. Pascher, R.H. Pearson, S. Sundell, Biochim. Biophys. Acta 650 (1981) 21–51.
[26] G. Büldt, J. Membr. Biol. 58 (1981) 81–100.
[27] G. Büldt, H.U. Gally, J. Seelig, G. Zaccai, J. Mol. Biol. 134 (1979) 673–691.
[28] H. Akatsu, Y. Kyoguki, H. Nakahara, K. Fukuda, Chem. Phys. Lipids 15 (1975) 222–230.
[29] P.L. Yeagle, W.C. Hutton, C. Huang, R.B. Martin, Biochemistry 16 (1977) 4344–4349.
[30] J.G. Vinter, A. Davis, M.R. Saunders, J. Comput. Aided Mol. Design 1 (1987) 31–51.
[31] P.B. Hitchcock, R. Mason, K.M. Thomas, G.G. Shipley, Proc. Natl. Acad. Sci. USA 71 (1974) 3036–3040.
[32] R.H. Pearson, I. Pascher, Nature 281 (1979) 499–501.